Front. Mater. Sci. 2023, 17(4): 230670
https://doi.org/10.1007/s11706-023-0670-8

RESEARCH ARTICLE

Preparation of a wearable K-PAN@CuS composite fabric with excellent photothermal/electrothermal properties

Jintao Zhang[1*], Qi Zhang[2*], Wei Pan (✉)[3,1], Yu Qi[1], Yajie Qin[1], Zebo Wang[4], and Jiarui Zhao[3]

1 International Joint Laboratory of New Textile Materials and Textiles of Henan Province, Zhongyuan University of Technology, Zhengzhou 450007, China
2 Huanghe Science and Technology College, Zhengzhou 450006, China
3 School of Materials and Chemical Engineering, Zhongyuan University of Technology, Zhengzhou 451191, China
4 College of Textiles, Zhongyuan University of Technology, Zhengzhou 451191, China

ABSTRACT: Electrospun nanofibers with highly efficient photothermal/electrothermal performance are extremely popular because of their great potential in wearable heaters. However, the lack of necessary wearable properties such as high mechanical strength and quick response of electrospun micro/nanofibers seriously affects their practical application. In this work, a technical route combining electrospinning and surface modification technology is proposed. The 3-triethoxysilylpropylamine-polyacrylonitrile@copper sulfide (K-PAN@CuS) composite fabric was achieved by modifying the original electrospinning PAN fiber and subsequently loading CuS nanoparticles. The results show that the break strength of the K-PAN@CuS fabric was increased by 10 times compared to that of the original PAN@CuS fabric. Furthermore, the saturated temperature of the K-PAN@CuS fabric heater could reach 116 °C within 15 s at a relatively low voltage of 3 V and 120.3 °C within 10 s under an infrared therapy lamp (100 W). In addition, due to its excellent conductivity, such a unique structural design enables the fiber to be closely attached to the human skin and helps to monitor human movements. This K-PAN@CuS fabric shows great potential in wearable heaters, hyperthermia, all-weather thermal management, and *in vitro* physical therapy.

KEYWORDS: electrospinning; strain sensor; electrothermal/photothermal conversion; CuS; wearable fabric

Contents

Received July 2, 2023; accepted November 7, 2023

E-mail: doctorpan0152@163.com

∗ J.Z. and Q.Z. contributed equally to this work.

1 Introduction

More and more researches are focused on flexible and wearable devices due to their potential applications in the fields of intelligent control of temperature, energy devices, sensor devices, health treatment, electrothermal therapy, etc. [1–4]. In recent years, wearable flexible heaters receive extensive attention as they require small size, lightweight, low cost, low power consumption, high strength, fast response speed, and durability to be used in various environments [5–7]. To meet the demands for those material properties during daily use, researchers are committed to developing multifunctional materials [8–9]. For instance, in the past decade, the performance of flexible optoelectronic devices has been significantly improved in the areas of energy storage, energy conversion, motion detection, and health therapy [10–12]. Nevertheless, comfort and wear resistance still need to be further improved. However, the inherent rigidity of film-based wearable devices limits their broad applications in wearable devices. To this end, various research approaches have been taken to develop fabric-based wearable electronic devices with varieties of conductive nanomaterials such as graphene, carbon nanotubes (CNTs), copper sulfide (CuS), and gold nanowires [13–17]. It is worth noting that CuS has been widely used in the field of energy conversion due to its high conductivity, good photothermal/electrothermal conversion performance, low cost, and simple preparation [18–20]. Therefore, it is of great significance to study all-weather flexible electronic devices not only with good photothermal/electrothermal conversion and wear resistance, but also with synergistic light and electric heating effects designed using nano-CuS as the functional filler. Meanwhile, this research also provides an effective reference for designing safe and durable wearable heaters.

With the wide application of electricity in life, heaters with Joule heating performance are becoming more and more popular. The preparation of wearable heaters with lightweight, fast voltage–temperature response, low voltage drive, good stability, and temperature controllability has become a research hotspot in the field of electrothermal wearable materials. Materials often used as conductive fillers include carbon materials (e.g., graphene and CNTs) [21–24] and metal nanoparticles (such as gold nanowires, silver nanoparticles, and copper) [25–29]. Zhang et al. [30] fabricated cotton fabrics coated with the prepared MXene, which exhibited excellent electrical conductivity, and their surface temperature reached 122 °C at 5 V, showing good thermal effect at a low voltage. Fan et al. [31] added CNTs into poly(amide–imide) (PAI) to prepare conductive polymer composites. Xu et al. [32] prepared cotton fabrics with excellent electrical and thermal conductivities by coating silver nanoparticles (AgNPs) and MXene. The surface resistance of the prepared fabric reached (23.4 ± 1.7) Ω/sq, and the surface temperature could reach 78 °C within 96 s under the driving voltage of 17.5 V. The fabric exhibited excellent electrical conductivity and electrical heating performance. Wang et al. [16] combined the composite layer of polydopamine (PDA)@CNT/AgNPs@CNT/PDA@CNT with the modified polyester fabric substrate to produce a flexible wear-resistant electronic fabric. The surface temperature reached 117 °C within 50 s under a voltage of 1.5 V. Although excellent Joule heating performance has been revealed in previous studies, high driving voltage and slow voltage response indicate the inability of those materials to meet the requirements of wearable heaters for safety and low energy consumption. Therefore, it is very important to prepare electric heaters with fast voltage–temperature response and low voltage drive.

Today and even in the future, humans will face a serious energy crisis, and the full utilization of energy has become a hot topic in related researches. This has also promoted the research and development of related scholars in the field of photothermal wearable materials. Cheng et al. [33] prepared a CuS/PDA-coated cotton fabric by chemical surface deposition providing excellent photothermal conversion and photocatalytic performance, which could quickly reach 90 °C in the light of a laser lamp with the density of 2 $W \cdot cm^{-2}$. Ren et al. [34] prepared silk fabric (SF)/chitosan quaternary ammonium salt (QCS)/CuS fabrics by treating SFs with CuS nanoparticles. The results showed that the prepared fabrics had almost perfect photothermal conversion effect

and the surface temperature could be rapidly increased to 98 °C under the laser irradiation with a density of 700 mW·cm^{-2}. However, the addition of conductive fillers often leads to the mechanical performance degradation of fibers. With attention to detail, photothermal materials on the fabric surface are easy to fall off during the long-term use, which will seriously deteriorate the performance of materials. In this context, developing flexible wearable intelligent fabrics with both high strength and excellent conductivity has important research value.

Meanwhile, the electrical driving methods of high-strength heaters based on flexible fabrics have been developed in recent years, which are used in the fields of electromagnetic interference shielding, human health physiotherapy [35–36], motion sensing [37], wearable electric heating clothing, etc. However, those electrothermal heaters cannot demonstrate their remarkable electrical heating performance without a power supply. Therefore, the development of fabric-based wearable heaters with fast thermal response, wide temperature range, and pluralistic driving energy source is crucial to adapting to various weather environments.

Electrospinning, a general technology for the preparation of micro/nanofibers, has many excellent properties such as large surface area, high aspect ratio, flexible surface function, and adjustable surface morphology [38–41]. At the same time, electrospinning has attracted widespread attention because of its simple operation and low cost. The porous electrospun fiber membrane has been proven to be a substrate for flexible devices with good air permeability. Among many electrospun polymers, polyacrylonitrile (PAN) is widely used due to its fiber formation, chemical stability, and corrosion resistance. On the other hand, with the rapid development of next-generation electronic devices, advanced thermal management has become the key to ensuring safe operation [42–44]. In general, crystalline materials such as metals, carbon-based materials and ceramics have high thermal conductivity [45]. However, the inherent rigidity itself of those materials hinders the further application of flexible electronics. To overcome this obstacle, nanocomposites composed of the insulating polymer matrix and inorganic fillers with high thermal conductivity are usually used to prepare flexible composites that integrate the mechanical stability of polymers and the high thermal conductivity of inorganic fillers [45–46]. In this study, CuS was *in situ* deposited on a electrospun PAN fabric by the chemical bath method (the optimal conditions for depositing CuS on a fabric by the chemical water bath method were completed in the previous study of the research group). The optimal ratio of CuS selected in this study was 3 wt.% (not repeated hereafter), and the PAN fibers were modified with the silane coupling agent, 3-aminopropyltriethoxysilane (KH-550). The uniform dispersion and firmness of CuS loaded on the fabric were significantly improved owing to the existence of intermolecular hydrogen bonds. The K-PAN@CuS reinforced electrothermal composites with high conductivity and good chemical stability were prepared. The application of K-PAN@CuS composites in intelligent wearable heaters and health monitors was studied from the perspective of the KH-550 crosslinking. The strength of the PAN@CuS fabric modified by 0.1 wt.% KH-550 was 1053% higher than that of the unmodified PAN@CuS one. Under a driving voltage of 3 V, the surface temperature of this compound rose rapidly to 116 °C within 15 s. This composite reveals excellent performance of low voltage, fast response, and high-efficiency electrothermal conversion. In addition, the excellent conductivity exhibited in this study endows K-PAN@CuS-containing devices with great application potential in the field of wearable smart sensors.

2 Experimental

2.1 Materials

PAN and KH-550 (analytical grade) were purchased from Nanjing Sandong Yousuo Chemical Technology Co., Ltd. Pentahydrate copper sulfate ($CuSO_4·5H_2O$, ⩾ 99%) and sodium thiosulfate pentahydrate ($Na_2S_2O_3·5H_2O$, ⩾ 99%) were from Xilong Scientific Co., Ltd., and acetic acid (CH_3COOH, 99.5%) was from Komio Chemical Reagent Co., Ltd., Tianjin. All these reagents were used directly without further purification. The deionized water used in this experiment was prepared in laboratory.

2.2 Instruments and characterization

The morphology and microstructure of the K-PAN@CuS fabric were observed by scanning electron microscopy (SEM) with an FEI Quanta 250 FEG microscope (USA). Possible functional groups in the sample were detected by Fourier transform infrared spectroscopy (FTIR) with a

spectrometer (Nicolet 560, Thermo Fisher Scientific, USA). X-ray diffraction (XRD) spectra were recorded using an X-ray diffractometer (DX-2700, Dandong Haoyuan Instrument Co., Ltd., China) in the 2θ range of 10°–70°. The resistivity of the sample was measured with a digital multimeter. The tensile strength and elongation at break of the samples were tested with an EUT2203 electronic universal tester. The sample to be tested was cut into a certain size (6 cm × 1 cm), and the thickness of the spline was tested with a digital millimeter. Three points were taken for each spline to calculate its average thickness, and each sample was tested five times.

2.3 Preparation of PAN fabrics

PAN (3.6 g) was dissolved in 27.4 g solution of dimethylformamide (DMF) at room temperature under magnetic stirring for 3 h to form a homogeneous spinning solution with the solid PAN content of approximately 12 wt.%. This precursor solution was then transferred into a 10 mL plastic syringe. The PAN fabrics were thereafter obtained by double-needle electrospinning for 9 h under following conditions: the applied voltage was 20 kV, the distance between the needle and the aluminum foil receiver was 10 cm, the feeding speed was 1 $mL \cdot h^{-1}$, and the ambient temperature and the humidity were controlled at 25 °C and 40%, respectively.

2.4 Surface modification of PAN fabrics

The acetic acid solution was first prepared with a concentration of 0.25%. Then four pre-prepared 0.25 wt.% acetic acid solutions of 100 mL each were added with 25, 50, 100 and 250 mg of KH-550, respectively. After KH-550 was completely dissolved by stirring with a magnetic stirrer for 1 h, the electrospun PAN fabrics were separately immersed in above solutions and left for 30 min aiming at modification. Finally, the PAN fabrics with different modification conditions were dried in a constant-temperature oven at 90 °C for 1 h, and the obtained fabrics were hereafter denoted as K-PAN-25, K-PAN-50, K-PAN-100, and K-PAN-250, respectively.

2.5 Preparation of K-PAN@CuS fabrics

K-PAN@CuS fabrics were prepared by a simple water bath deposition method. Briefly, a certain amount of $CuSO_4 \cdot 5H_2O$ and $Na_2S_2O_3 \cdot 5H_2O$ weighed at a molar ratio of 1:1 were added into deionized water. Then the modified PAN fabrics were immersed into the beaker containing above solution and slowly heated to 80 °C for 2 h. The K-PAN@CuS fabrics with different contents of KH-550 (0.025, 0.05, 0.1, and 0.25 wt.%) were finally prepared by sonication for 3 min and dried at 60 °C for 1 h, which were hereafter denoted as K-PAN@CuS-25, K-PAN@CuS-50, K-PAN@CuS-100, and K-PAN@CuS-250, respectively. A schematic diagram for the modification of the K-PAN@CuS fabric is shown in Fig. 1.

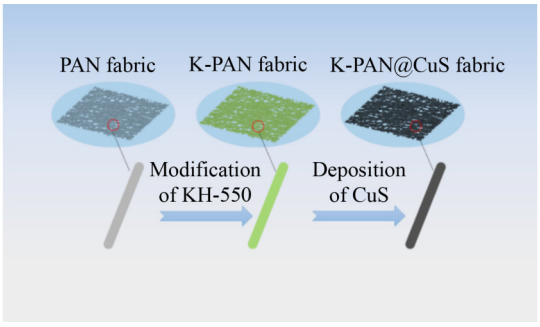

Fig. 1 Schematic demonstration for the preparation of the K-PAN@CuS fabric.

2.6 Electrothermal and stability characterization

Firstly, the as-prepared K-PAN@CuS fabric was cut into a rectangular shape of 3 cm × 2 cm. Then, two conductive clamps were fixed firmly at both ends of the K-PAN@CuS fabric and placed horizontally on a foam board to eliminate the heat dissipation during heating. The electric heating performance of the K-PAN@CuS fabric under a specific voltage was also studied using a power supply (MS-155D, Maxon), and an infrared thermal imager (FLIR, E60) was used to record temperature change of the sample surface. Furthermore, the distance between the thermal imager and the experimental sample was always maintained at 30 cm.

2.7 Photothermal characterization

The K-PAN@CuS fabric (4 cm × 4 cm) was placed horizontally on a melamine plate. Afterwards, an infrared therapy lamp (100 W) was used as the light source to vertically irradiate the sample, and the temperature change of the sample surface was recorded by an infrared thermal imager (FLIR, E60).

3 Results and discussion

3.1 Preparation and characterization of K-PAN@CuS fabrics

Generally, weak interaction between PAN fibers may lead to unsatisfactory mechanical properties of the fibers. Therefore, it is necessary to modify PAN fibers in order to improve their strength. KH-550 is a typical coupling agent, the surface of which contains a great number of functional groups that can achieve the purpose of modifying the matrix material. The preparation process of the K-PAN@CuS fabric is shown in Fig. 1. As mentioned above, there are possible changes in the above preparation process, which are also revealed in Fig. 2. Firstly, the alkoxide group ($-OCH_2CH_3$) in the silane coupling agent KH-550 was hydrolyzed into the hydroxyl group ($-OH$) under acidic conditions [47]. Secondly, the nitrile group in PAN fibers interacted with the amino group in KH-550. Finally, the nitrile and hydroxyl groups in partially cross-linked PAN fabrics were combined with Cu^{2+} by coordination, thus firmly depositing CuS particles on the surface of PAN fabrics [48]. The whole formation process of CuS nanosheets could generally be recorded as Eqs. (1)–(3):

$$S_2O_3^{2-} + H_2O \rightarrow SO_4^{2-} + H_2S \quad (1)$$

$$H_2S + Cu^{2+} \rightarrow CuS\downarrow + 2H^+ \quad (2)$$

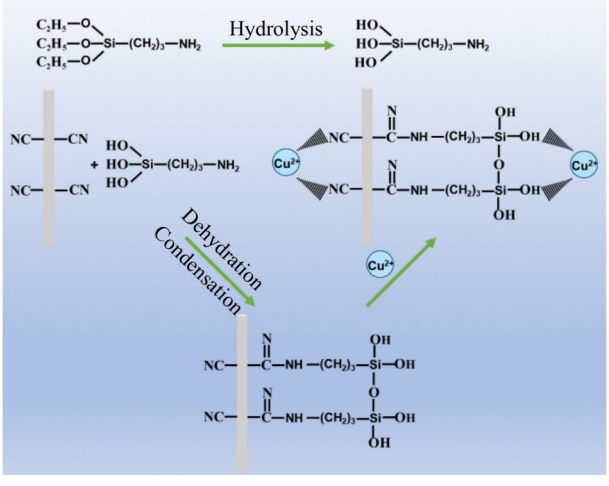

Fig. 2 Schematic illustration of the CuS deposition on the PAN fabric.

$$nCuS \rightarrow (CuS)_n \quad (3)$$

The FTIR spectra are illustrated in Fig. 3(a). For the original PAN, the band at 3436 cm^{-1} is assigned to the $-OH$ stretching vibration mode, while the band at 2248 cm^{-1} is associated with the C≡N stretching vibration. The distinct peak at 2924 cm^{-1} is related to the C−H stretching vibration. The absorption band appears at 1450 cm^{-1} due to the bending deformation of C−H [48]. It should be noted that after the treatment with KH-550, new bands can be seen in the K-PAN fabric. The characteristic −CN peak at 2248 cm^{-1} is weakened, which may result from the modification between the PAN fiber and the KH-550 couple agent. Besides, the bending at 617 cm^{-1} corresponds to the Cu−S bending mode. However, the peak at 2248 cm^{-1} is weakened or even completely disappears due to the interaction between Cu^{2+} and −CN groups [48], which also strongly proves the successful preparation of the modified K-PAN@CuS fabric. To further analyze the crystalline structural change under the modification by the coupling agent KH-550, XRD was performed and the results are shown in Fig. 3(b). It is observed that all samples have diffraction peaks at 2θ = 17° [49–51] that correspond to the crystallization peaks of the PAN fabric, implying that the crystal structure of the PAN fiber is unchanged after the KH-550 modification and the CuS deposition. Furthermore, seven additional diffraction peaks at the 2θ values of 27.8°, 29.5°, 31.9°, 32.9°, 47.9°, 52.7° and 59.3° are derived from (1 0 1), (1 0 2), (1 0 3), (1 0 6), (1 1 0), (1 0 8) and (1 1 6) planes, respectively, consistent with the standard data of CuS (JCPDS card no. 06-0464) [14,52].

The morphology of the PAN fabric with a diameter of (110 ± 20) nm is revealed in Fig. 4(a). The original PAN fiber with smooth surface and nanoscale size could be prepared by electrospinning. For the K-PAN fabric after the modification, its surface becomes rough and the fibers become thicker due to the presence of silanol groups formed by the dehydration reaction between KH-550 and hydroxyl groups absorbed onto the PAN fabric. It is composed of partially cross-linked fibers. In addition, the K-PAN fabric, as a surface-modified material, also provides numerous active sites for the deposition of CuS functional nanoparticles, which is proven by Fig. 4(c) that the K-PAN fabric surface is uniformly covered with CuS nanoparticles chemically deposited, forming a uniform conductive layer with the capability to enhance the conductivity without sacrificing the strength and

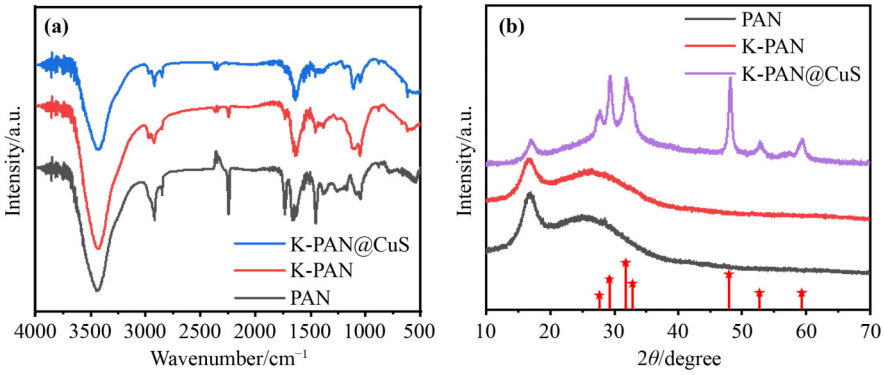

Fig. 3 (**a**) FTIR spectra of original PAN, K-PAN, and K-PAN@CuS. (**b**) XRD patterns of original PAN, K-PAN, and K-PAN@CuS.

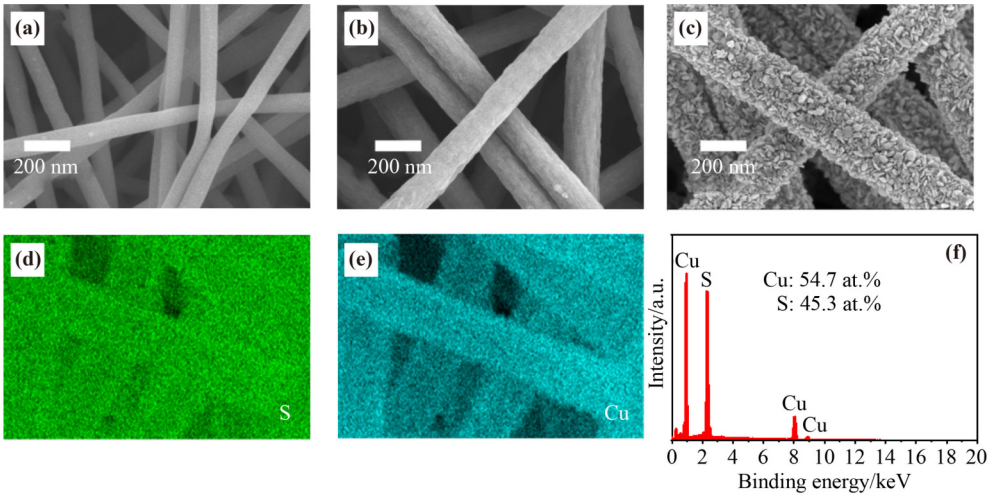

Fig. 4 SEM images of (**a**) original PAN fabric, (**b**) K-PAN fabric, and (**c**) K-PAN@CuS fabric. (**d**)(**e**) Elemental mapping images of S and Cu and (**f**) EDS analysis result of the K-PAN@CuS fabric.

gentleness. The elemental mapping images of S and Cu in the K-PAN@CuS fabric are shown in Figs. 4(d) and 4(e), respectively, from which it is seen that CuS is uniformly deposited onto the K-PAN fiber. Moreover, the corresponding energy dispersive spectroscopy (EDS) analysis result of the K-PAN@CuS fabric, as presented in Fig. 4(f), also confirms the successful coating of CuS nanocrystals on the modified K-PAN fabric.

3.2 Mechanical performances of K-PAN@CuS fabrics

It has important application value to evaluate the mechanical performances of the fabrics. Figure 5(a) reveals the tensile mechanical properties of the composite fabric membranes. Compared with that of the original PAN fiber, the strengths of all K-PAN fibers are enhanced. It is notable that the strength of the PAN fiber modified with 0.1 wt.% KH-550 reaches 9.31 MPa. Since the strength of the original PAN fabric is only 3.36 MPa, the strength of this modified fiber increases by 177%, while its elongation at break also increases by 42%. The improvement of the fabric strength is mainly related to the force among fibers modified by the silane coupling agent KH-550. After the chemical deposition of CuS, the strength of the K-PAN@CuS fabric first rises and then drops with the increase of the modifier concentration, as shown in Fig. 5(b). It is observed that the K-PAN@CuS-100 fabric has the best mechanical performance among all K-PAN@CuS samples, with the strength and the elongation at break of 5.65 MPa and 18%, respectively, needless to say, much higher than those of the pristine PAN@CuS fabric with the break strength of 0.49 MPa and the elongation at break of 11%. The intrinsically good flexibility and mechanical strength of PAN as well as the interfacial interactions between KH-550 and PAN render the K-PAN@CuS-100 fabric excellent flexibility

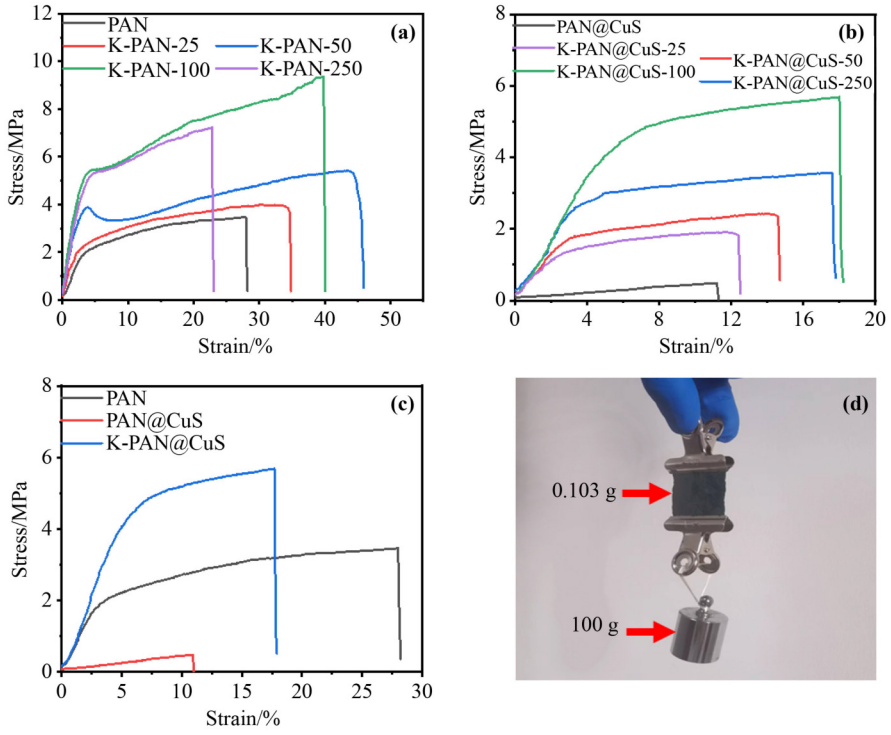

Fig. 5 (**a**) Stress–strain curves of untreated and treated PAN fiber with different concentrations of KH-550. (**b**) Stress–strain curves of untreated and treated PAN@CuS fiber with different concentrations of KH-550. (**c**) Stress–strain curves of PAN, PAN@CuS and K-PAN@CuS. (**d**) Photograph of 0.103 g K-PAN@CuS-100 nanofiber membrane withstanding a weight of 100 g.

including bendability, foldability, twistability, and even rollability. It is also detected from Fig. 5(d) that the lightweight K-PAN@CuS-100 film of only 0.103 g easily hold a weight of up to 100 g without breaking, further demonstrating its high mechanical strength.

3.3 Electrothermal characterization of K-PAN@CuS fabrics

Because the electrospun PAN fabric is an electrically insulating material, the chemical deposition of conductive particles can be considered to improve its conductivity. The densities and firmness of CuS deposited on the fabrics with different modifier concentrations are obviously different (Fig. S1(c)). Figure 6(a) shows that with the increase of the KH-550 content from 0 to 0.25 wt.%, the conductivity of the sample upgrades from 21.3 to 247.3 $S \cdot m^{-1}$. Meanwhile, the weight gain rate of the K-PAN@CuS fabric is also found to rise from 71% to 128% as depicted in Fig. S2. All these results show that the K-PAN@CuS fabric has excellent electrical conductivity, providing the potential in the manufacture of Joule-heated electric heaters. Besides, considering the effect of the KH-550 content on the strength of K-PAN@CuS fabrics, the K-PAN@CuS-100 fabric is selected as the representative of the next feature of those K-PAN@CuS fabrics. Figure 6(b) shows time-dependent variations of temperature for K-PAN@CuS-100 at different driving voltages (0.5–3 V). It is seen that the K-PAN@CuS-100 fabric has an extremely rapid response to the electrothermal conversion, and the surface temperature rapidly reaches saturation in around 15 s. The electric heating fabric shows a steady-state temperature as high as 116 °C at a low voltage of 3 V. Furthermore, the surface saturation temperatures of the sample reach 28.1, 34.2, 43.6, 56.1 and 73.3 °C at the voltages of 0.5, 1, 1.5, 2 and 2.5 V, respectively, based on which it can be deduced that the surface saturation temperature increases sharply with the voltage rise. To achieve the comfort of the electric heating fabric, it is necessary to realize the real-time controllability of the heating temperature. Therefore, the sensitivity of the heating process is an important parameter of the flexible electric heater. Figure 6(c) shows the instantaneous temperature evolution of the K-PAN@CuS-100 fabric under different driving voltages, in which the illustrations depict the surface temperature distributions of the K-PAN@CuS-100 fabric when the temperature is stable. The fabric can achieve a

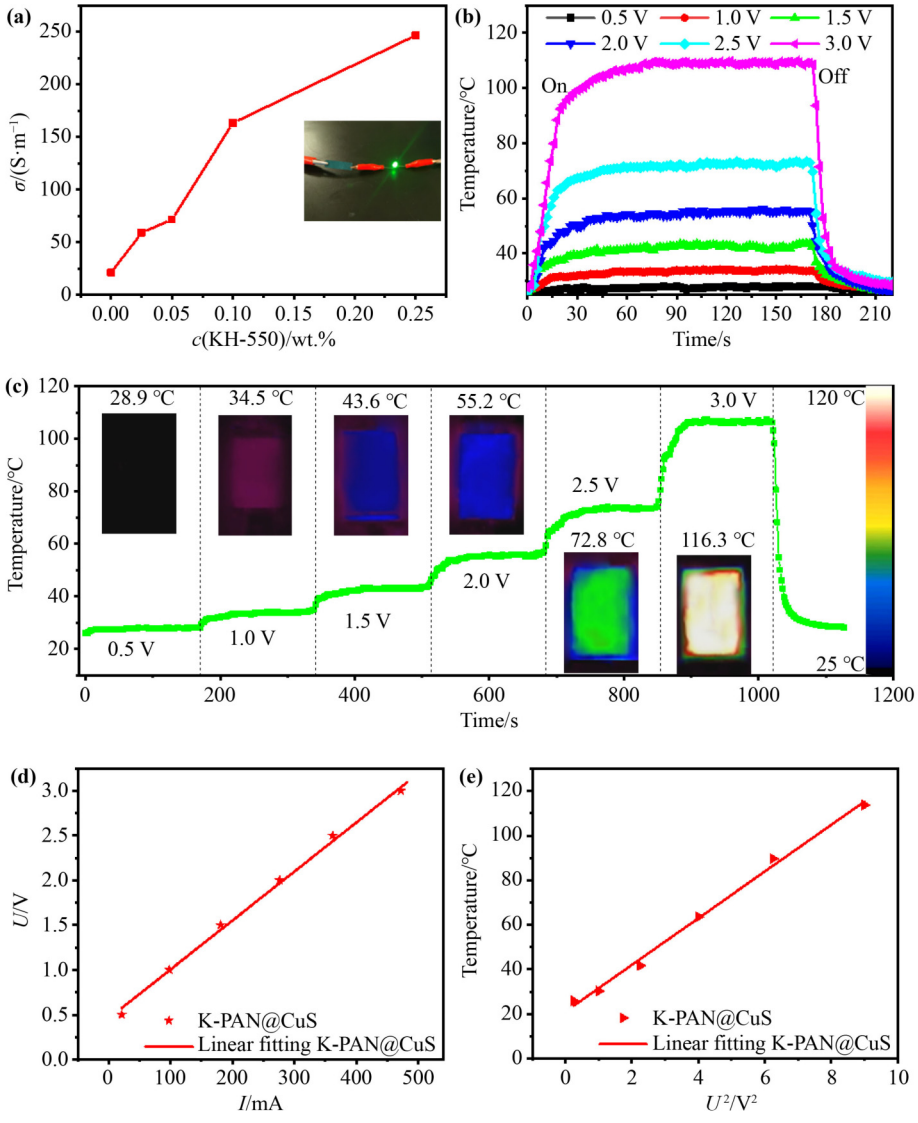

Fig. 6 (**a**) Experimental measurement of the conductivity for K-PAN@CuS fabrics with different concentrations of KH-550 (inset is an LED bulb lit up using the K-PAN@CuS-100 conductive wire). (**b**) Transient temperature evolution of the K-PAN@CuS-100 fabric at various voltages. (**c**) Instantaneous temperature evolution process of the PAN@CuS-100 fabric at various voltages. (**d**) *U*–*I* and (**e**) T–U^2 curves of the K-PAN@CuS-100 fabric.

controllable temperature range of 28–116 °C in the low-voltage range of 0.5–3 V, implying a high response sensitivity. The infrared thermal imaging in this work reveals the uniform temperature distribution on the surface of the K-PAN@CuS-100 fabric, which has a wide application prospect in the field of intelligent control on wearable devices.

The fine linear relationship between voltage and current in Fig. 6(d) indicates the temperature controllability of the material as a flexible electric heater. It is an important indicator to guarantee the safe working of wearable heaters in the human body. The linear fitting of U^2 and the surface saturation temperature T in Fig. 6(e) provides the possibility of accurately predicting the saturation temperature at a specific voltage. The lower driving voltage of the K-PAN@CuS-100 fabric can ensure safety of the wearing process.

To better understand the mechanism of electrically driven Joule heaters, the electrically heating response for the K-PAN@CuS-100 fabric was analyzed in detail. According to the energy balance theorem, the saturation temperature of the heater was evaluated. In brief, the saturated surface temperature would be obtained when the dissipated power through the Joule heater became equal to the energy loss by conduction, radiation, and convection. Specifically, the temperature of the nanofiber would be

calculated through the following equation:

$$\frac{U^2}{R} = mc\frac{\mathrm{d}T}{\mathrm{d}t} + hA(T - T_0) \quad (4)$$

where U is the supplied voltage, R is the resistance of the heating device, c is the specific heat capacity, m is the weight of the compound, T is the saturated temperature of the film surface, T_0 is the original temperature, t is the heating time, A represents the effective heating area, and h is the heat-transfer coefficient. According to Eq. (4), the surface temperature (T) of the K-PAN@CuS-100 heater can be obtained by linear fitting on U^2 [53].

In addition, the stability and wear resistance of the electrothermal conversion are important factors influencing the reuse of the K-PAN@CuS-100 fabric. Figure S3 shows the resistance changes of the K-PAN@CuS-100 fabric during the bending at different angles (Fig. S3(a)) and during the multiple bending to the same angle of 90° with different cycle numbers (Fig. S3(b)). The test results indicate that the fabric resistance does not change significantly with the variations of the bending angle and the bending cycle number, implying its excellent resistance stability. Figure 7(a) reveals the repeatability test result of the K-PAN@CuS-100 fabric through 15 switching cycles at an applied voltage of 3 V. It can be seen that when the same voltage is repeatedly applied, the saturation temperature of the material surface responds quickly, and the curve remains almost unchanged during 15 cycles. Figure 7(b) shows temperature–time curves of the sample at the first, fifth, tenth, and fifteenth cycles, which almost coincide, meaning that the sample has excellent heating-temperature reproducibility and durability. Figure 7(c) shows the long-term temperature–time curve of K-PAN@CuS-100 recorded in the test duration of 1 h. It is detected that the saturation temperature of the material fluctuates at (118 ± 3) °C under the driving voltage of 3 V, showing the potential for long-term heating with stability.

In the application of flexible wearable electric heaters, the influence of the bending mode on electric heating behaviors of the material should be considered as an important factor. Figure 8(a) shows a photograph and corresponding infrared (IR) images of the K-PAN@CuS-100 fabric under different bending modes. It is clear that the surface temperature of the electric heater does not change significantly at 2 V, which means that the bending mode does not have an obvious influence on the

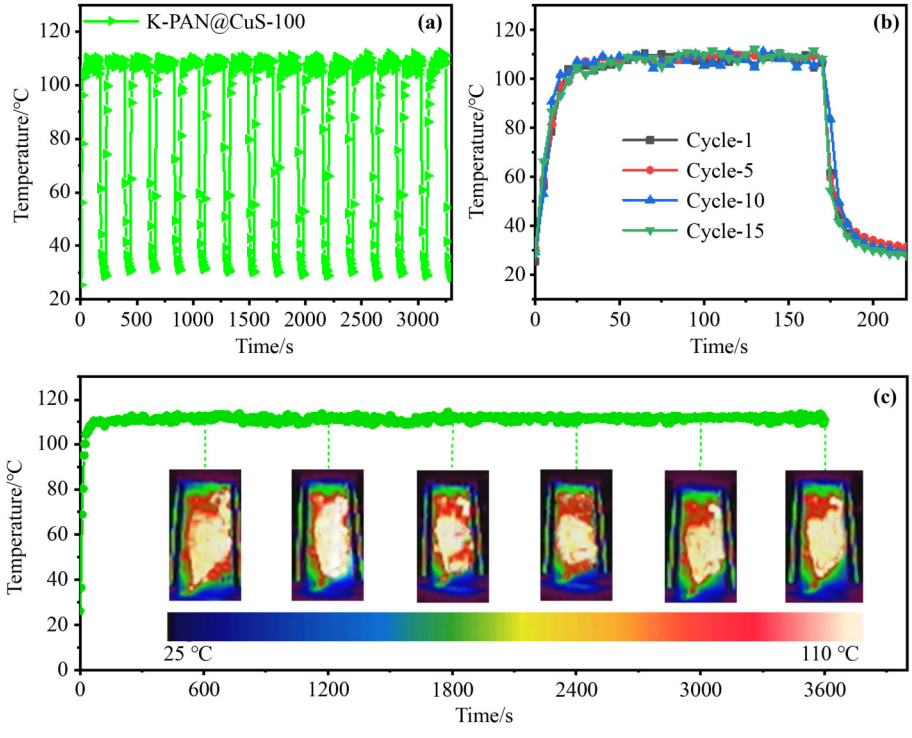

Fig. 7 (**a**) Electrothermal cycling stability of the K-PAN@CuS-100 fabric at an applied voltage of 3 V. (**b**) Electrical heating stability during the 1st, 5th, 10th, and 15th cycles at 3 V. (**c**) Long-term heating test result for the K-PAN@CuS-100 fabric at 3 V and corresponding IR images.

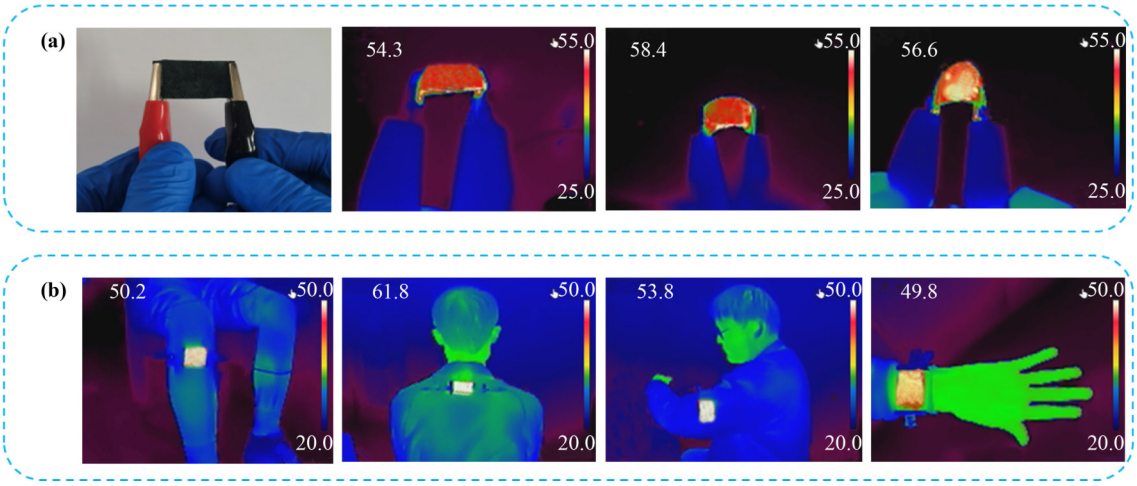

Fig. 8 (**a**) A digital photo and IR camera images of the as-prepared K-PAN@CuS-100 fabric under different bending modes. (**b**) Electrothermal wearable performance of the K-PAN@CuS-100 fabric under 2 V.

temperature distribution of this fabric, indicating its excellent Joule thermal stability and uniform heating performance. It is worth noting that the surface temperature of the K-PAN@CuS-100 electric heater rapidly reaches 55 °C at a relatively low driving voltage, indicating its application potential in the area of wearable Joule heaters. Therefore, in this study, we provide the prepared K-PAN@CuS-100 fabrics (4 cm × 6 cm) for wearable devices to be worn on stomach, cervical vertebrae, arm and wrist for thermal therapy. Figure 8(b) presents IR images of fabric devices worn on the body, indicating that the surface temperature increase rapidly from 25 to 52 °C within 15 s under the relatively low-voltage drive of 2 V, regardless of the fabric shape. The above experiments prove that the K-PAN@CuS-100 fabric, as an electric heater, has fast temperature response and precise temperature control, which can achieve local temperature thermotherapy, suggesting its feasibility of the application in wearable devices for thermal therapy and body warming.

3.4 Application of K-PAN@CuS fabrics in flexible wearable strain sensors

Another noteworthy aspect of the K-PAN@CuS-100 fabric is its promising application in flexible strain sensors. As shown in Fig. S4, the $(R-R_0)/R_0$ value of the fabric increases with the enhancement of the strain, owing to that the density of CuS conductive particles rises while the resistance drops during the stretching process. To further investigate the potential application of the K-PAN@CuS-100 fabric as a strain sensor, the gauge factor (GF) of the material was tested by Eq. (5) [54–55]:

$$\mathrm{GF} = \frac{R - R_0}{R_0 \varepsilon} \tag{5}$$

where R is the resistance in the stretched state, R_0 is the initial resistance, and ε is the applied strain. The result shows that there is an obvious linear relationship between $(R-R_0)/R_0$ and the strain of the material. By calculation, the GF value of the fabric 5.22 is obtained, which indicates that the K-PAN@CuS-100 fabric has high sensitivity. Some demonstration experiments have been carried out to reveal the sensing capability of the K-PAN@CuS-100 fabric sensor with the resulted corresponding curves of $(R-R_0)/R_0$ versus time depicted in Fig. 9. It shows that the K-PAN@CuS-100 fabric as a sensor mounted on the mask has the capability to detect resistance changes in the breathing rate at different times. These tests are applicable to detect both weak stresses (normal breath, deep breath, swallow) and intense exercises (finger bending, wrist bending, elbow bending). For instance, as shown by Figs. 9(a) and 9(b), the sensor can be attached onto the mask easily for the recognition of different breathing patterns of the human body. In addition, the K-PAN@CuS-100 fabric sensor can also identify large movements. Moreover, the K-PAN@CuS-100 fabric sensor has been attached to elbow, wrist and finger for bending recognition. Figures 9(d) and 9(e) depict curves of $(R-R_0)/R_0$ versus time that reflect the response from different parts of the body. It is observed that with the increase of the deformation, there is an increment of the relative resistance change. After the completion of different actions, the sensor shows high

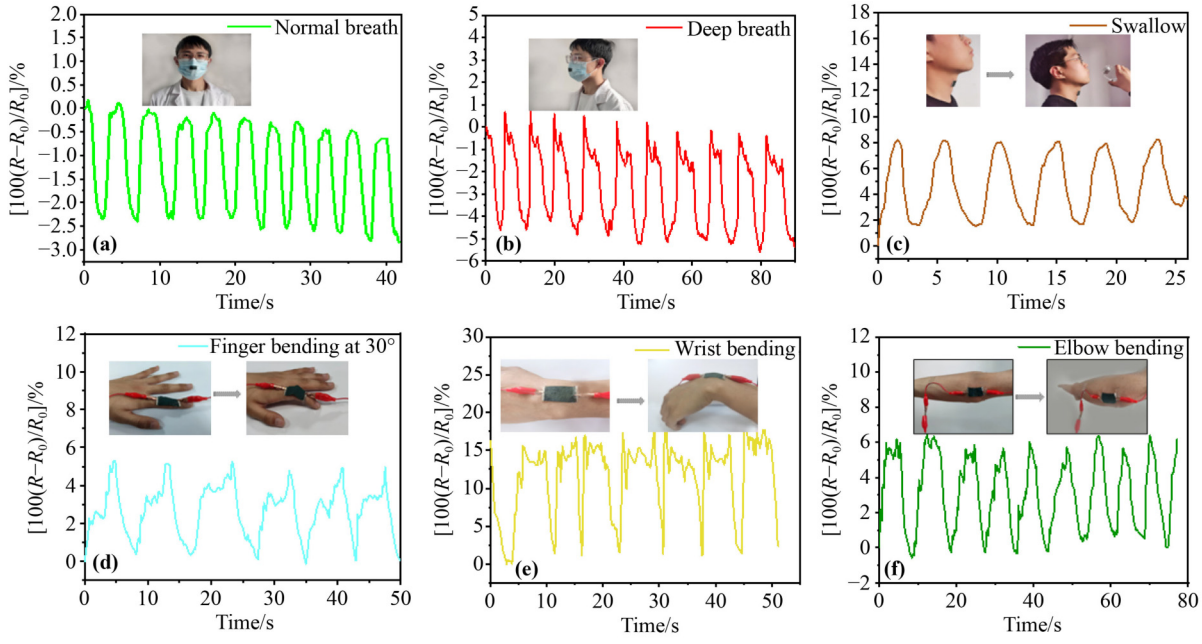

Fig. 9 Detection of various human motions using the wearable K-PAN@CuS-100 strain sensors with resulting photographs and corresponding signal variations from wearable sensors to reveal (**a**) normal breath, (**b**) deep breath, (**c**) swallow, (**d**) finger bending at 30°, (**e**) wrist bending, and (**f**) elbow bending.

flexibility and reliability for the human motion detection. In order to better evaluate its durability and reliability, the fabric has been subjected to finger bending at 30° for 200 cycles. As shown in Fig. S5, the $(R-R_0)/R_0$ signal possesses high regularity and consistence. From above results, it can be seen that CuS endows the PAN fabric with intelligent sensing, excellent strength, and wearable application. The strain sensor assembled by this material thus has great application value in personal motion feedback and patient rehabilitation.

3.5 Photothermal performance

CuS nanoparticles have been proven to own the consummate photothermal conversion ability [53], which is hoped to endow PAN fabrics with excellent photothermal performance. This is an effective way for Joule heaters to meet the needs of heating applications when there is no power supply. In this work, the photothermal ability of the K-PAN@CuS-100 fabric (4 cm × 4 cm) has been revealed by its exposure to an IR therapy lamp with the power of 100 W, and Fig. 10(b) presents surface temperature–time curves of the K-PAN@CuS-100 fabric at different distances away from the irradiation, which indicates the rapid photothermal response as well as the negative correlation between the saturation temperature of the fabric and the light source distance away from the fabric. The saturated temperature of K-PAN@CuS-100 can reach up to 120.3 °C within 10 s at a distance of 30 cm, and then quickly drops to the air temperature once the light source is turned off. Additionally, when the distance between the K-PAN@CuS-100 fabric and the light source is up to 50 cm, the surface saturation temperature can still reach 70.3 °C in just 10 s. Compared with those of some fabrics reported in recent years, the K-PAN@CuS-100 fabric revealed in this work has improved photothermal conversion performance, which are summarized in Table S1 [56–60]. Figure 10(c) presents IR images depicting distribution of the saturation temperature on the fabric surface at different distances away from the light source. When the photothermal conversion fabric (6 cm × 6 cm) is worn on the knee, its temperature increases to 56.7 °C at a distance of 80 cm from the irradiation, as illustrated in Fig. 10(d).

Cyclic heating and cooling tests have also been carried out to investigate the photothermal stability of the K-PAN@CuS-100 fabric. It is observed from Fig. 10(e) that the surface temperature of the fiber responds rapidly and there are nearly overlapped cycle curves till the 10th cycle, demonstrating that the cyclic light heating performance is stable. In addition, the long-term light heating stability of the flexible fiber is also an important reference standard for evaluating its performance. As depicted in Fig. 10(f), the fabric surface temperature can

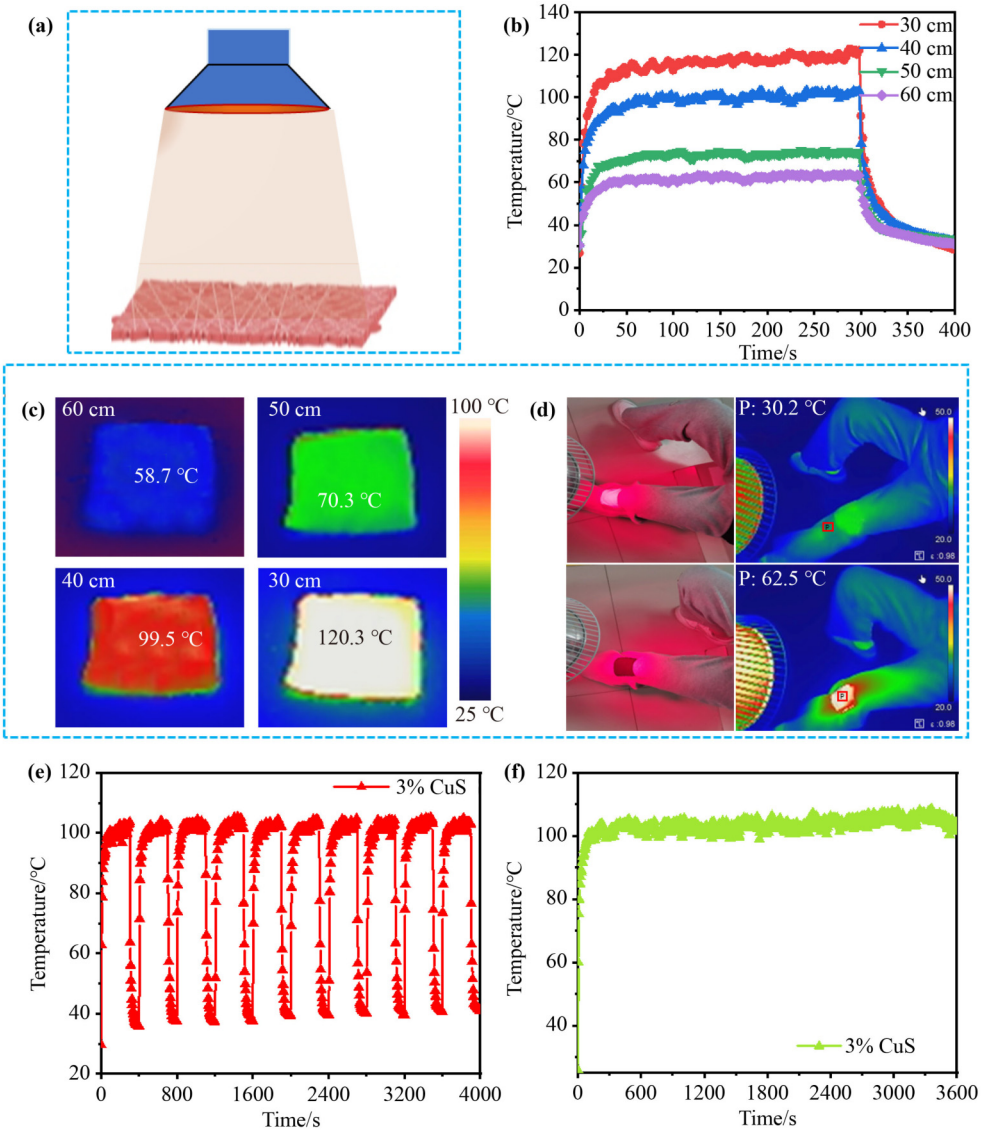

Fig. 10 (**a**) Schematic of the K-PAN@CuS-100 fabric photothermally tested by IR therapy lamp. (**b**) Temperature–time curves of the K-PAN@CuS-100 fabric at different distances from the light source. (**c**) IR images of the K-PAN@CuS-100 fabric at different distances from the light source. (**d**) Wearable applications of the K-PAN@CuS-100 fabric (6 cm × 6 cm) at the distance of 80 cm from the light source. (**e**) Cyclic stability and (**f**) temperature stability of the K-PAN@CuS-100 fabric under the light for a relatively long duration.

remain stable under light for a duration of more than 3600 s, proving its excellent heating stability.

In addition, to further study the photothermal conversion performance of the K-PAN@CuS-100 fabric, we put them in direct sunlight at 11:00, 14:00 and 16:00, and the surface temperature evolution curves of the fabric with time were recorded using a thermal imager. As shown in Fig. S6(a), the surface temperatures of the K-PAN@CuS-100 fabric rise rapidly and reach stabilization within 50 s. At the time points of 11:00 and 14:00, the steady-state temperatures of the fabric reach 50.5 and 62.3 °C, respectively. In addition, the solar photothermal images at different time points in Fig. S6(b) show the uniform temperature distributions on the K-PAN@CuS-100 fabric, which further confirms its potential application in the wearable thermal management.

4 Conclusions

In this work, photothermal/electrothermal K-PAN@CuS fabrics-based heaters are fabricated through electrospinning and chemical bath deposition. The silane coupling agent (KH-550) is chosen as the modifier of the PAN

fabric. The mechanical strength of the K-PAN@CuS fabric has been greatly improved (9.31 MPa) by the modification of the coupling agent KH-550. Compared with the original PAN@CuS fabric, the break strength of the K-PAN@CuS fabric is increased by 10 times. Meanwhile, the conductive layer is located at the outer frame, giving the fabric excellent flexible electrical conductivity. Such a unique structural design enables the fiber to be closely attached to the human skin and helps to monitor human movements. In addition, the K-PAN@CuS fabric can also be used for light/electric heating. The saturated temperature of the K-PAN@CuS fabric heater can reach 116 °C within 15 s at a relatively low voltage of 3 V, while the surface temperature can reach 120.3 °C within 10 s under the IR therapy lamp (100 W). In summary, the K-PAN@CuS fabric exhibits fast response, long-term stability, and stable photothermal/electrothermal performances. This fabric with excellent electrical and mechanical properties might have great practical application potential in the field of wearable electronic devices.

Declaration of competing interests The authors declare that they have no competing financial interests.

Acknowledgements The authors gratefully acknowledge the financial support from the Key Science and Technology Project of Henan Province (Grant No. 222102230093).

Electronic supplementary information Supplementary materials can be found in the online version at https://doi.org/10.1007/s11706-023-0670-8 and https://journal.hep.com.cn/foms/EN/10.1007/s11706-023-0670-8, which include Figs. S1–S6 and Table S1.

References

[1] Li S, Zhang Y, Wang Y, et al. Physical sensors for skin-inspired electronics. InfoMat, 2020, 2(1): 184–211

[2] Chao M, Wang Y, Ma D, et al. Wearable MXene nanocomposites-based strain sensor with tile-like stacked hierarchical microstructure for broad-range ultrasensitive sensing. Nano Energy, 2020, 78: 105187

[3] Agcayazi T, Chatterjee K, Bozkurt A, et al. Flexible interconnects for electronic textiles. Advanced Materials Technologies, 2018, 3(10): 1700277

[4] Lee S J, Kim C L. Highly flexible, stretchable, durable conductive electrode for human-body-attachable wearable sensor application. Polymer Testing, 2023, 122: 108018

[5] Wang B, Facchetti A. Mechanically flexible conductors for stretchable and wearable E-skin and E-textile devices. Advanced Materials, 2019, 31(28): 1901408

[6] Cai G, Yang M, Xu Z, et al. Flexible and wearable strain sensing fabrics. Chemical Engineering Journal, 2017, 325: 396–403

[7] He P, Pu H, Li X, et al. CNTs-coated TPU/ANF composite fiber with flexible conductive performance for joule heating, photothermal, and strain sensing. Journal of Applied Polymer Science, 2023, 140(13): e53668

[8] Wang S, Chen W, Wang L, et al. Multifunctional nanofiber membrane with anti-ultraviolet and thermal regulation fabricated by coaxial electrospinning. Journal of Industrial and Engineering Chemistry, 2022, 108: 449–455

[9] Wang H, Ma Y, Qu J, et al. Multifunctional PAN/Al–ZnO/Ag nanofibers for infrared stealth, self-cleaning, and antibacterial applications. ACS Applied Nano Materials, 2022, 5(1): 782–790

[10] Wu F, Tian Z, Hu P, et al. Lightweight and flexible PAN@PPy/Mxene films with outstanding electromagnetic interference shielding and joule heating performance. Nanoscale, 2022, 14(48): 18133–18142

[11] Qi H, Yang L, Tang X, et al. Electrospun light stimulus response-enhanced anisotropic conductive Janus membrane with up/down-conversion luminescence. Materials Chemistry Frontiers, 2022, 6(16): 2219–2232

[12] Liu Z, Tian B, Liu X, et al. Multifunctional nanofiber mat for high temperature flexible sensors based on electrospinning. Journal of Alloys and Compounds, 2023, 941: 168959

[13] Al-Hamry A, Lu T, Bai J, et al. Versatile sensing capabilities of layer-by-layer deposited polyaniline-reduced graphene oxide composite-based sensors. Sensors and Actuators B: Chemical, 2023, 390: 133988

[14] Liu B, Zhang Q, Huang Y, et al. Bifunctional flexible fabrics with excellent joule heating and electromagnetic interference shielding performance based on copper sulfide/glass fiber composites. Nanoscale, 2021, 13(44): 18558–18569

[15] Svyntkivska M, Makowski T, Shkyliuk I, et al. Electrically conductive crystalline polylactide nonwovens obtained by electrospinning and modification with multiwall carbon nanotubes. International Journal of Biological Macromolecules, 2023, 242: 124730

[16] Wang X, Li T Y, Geng W H, et al. Flexible wearable electronic fabrics with dual functions of efficient EMI shielding and electric heating for triboelectric nanogenerators. ACS Applied Materials & Interfaces, 2023, 15(18): 22762–22776

[17] Wang Y, Chen J, Shen Y, et al. Control of conductive and mechanical performances of poly(amide–imide) composite films utilizing synergistic effect of polyaniline and multi-walled carbon nanotube. Polymer Engineering and Science, 2019, 59(s2): E224–E230

[18] Xiong F, Yuan K, Aftab W, et al. Copper sulfide nanodisk-doped

solid–solid phase change materials for full spectrum solar-thermal energy harvesting and storage. ACS Applied Materials & Interfaces, 2021, 13(1): 1377–1385

[19] Singh N. Copper(II) sulfide nanostructures and its nanohybrids: recent trends, future perspectives and current challenges. Frontiers of Materials Science, 2023, 17(3): 230632

[20] Kim M R, Hafez H A, Chai X, et al. Covellite CuS nanocrystals: realizing rapid microwave-assisted synthesis in air and unravelling the disappearance of their plasmon resonance after coupling with carbon nanotubes. Nanoscale, 2016, 8(26): 12946–12957

[21] Liu P, Li Y, Xu Y, et al. Stretchable and energy-efficient heating carbon nanotube fiber by designing a hierarchically helical structure. Small, 2018, 14(4): 1702926

[22] Jang H S, Jeon S K, Nahm S H. The manufacture of a transparent film heater by spinning multi-walled carbon nanotubes. Carbon, 2011, 49(1): 111–116

[23] Xue C H, Du M M, Guo X J, et al. Fabrication of superhydrophobic photothermal conversion fabric via layer-by-layer assembly of carbon nanotubes. Cellulose, 2021, 28(8): 5107–5121

[24] Zhao Y, Meng Y, Yu P, et al. Modified reduced graphene oxide-LDH/WPU nanohybrid coated nylon 6 fabrics for durable photothermal conversion performance. Applied Surface Science, 2023, 622: 156900

[25] Bhattacharjee S, Macintyre C R, Bahl P, et al. Reduced graphene oxide and nanoparticles incorporated durable electroconductive silk fabrics. Advanced Materials Interfaces, 2020, 7(20): 2000814

[26] Li H, Pan Y, Du Z. Self-reduction assisted MXene/silver composite tencel cellulose-based fabric with electrothermal conversion and NIR photothermal actuation. Cellulose, 2022, 29(15): 8427–8441

[27] Zhang Y, Su H, Li H, et al. Enhanced photovoltaic–pyroelectric coupled effect of $BiFeO_3$/Au/ZnO heterostructures. Nano Energy, 2021, 85: 105968

[28] Ly T N, Park S. Wearable strain sensor for human motion detection based on ligand-exchanged gold nanoparticles. Journal of Industrial and Engineering Chemistry, 2020, 82: 122–129

[29] Zhang Y, Ren H, Chen H, et al. Cotton fabrics decorated with conductive graphene nanosheet inks for flexible wearable heaters and strain sensors. ACS Applied Nano Materials, 2021, 4(9): 9709–9720

[30] Zhang H, Ji H, Chen J, et al. A multi-scale MXene coating method for preparing washable conductive cotton yarn and fabric. Industrial Crops and Products, 2022, 188: 115653

[31] Fan Z, Wang Y, Jeon J, et al. Enhancing multiwalled carbon nanotubes/poly(amide–imide) interfacial strength through grafting polar conjugated polymer on multiwalled carbon nanotubes. Surfaces and Interfaces, 2022, 32: 102130

[32] Xu Q, Wang X, Zhang Y, et al. Temperature-controlled wearable heater of durably conductive cotton fabric prepared by composite coatings of silver/MXene and polydimethylsiloxane. Applied Surface Science, 2023, 625: 157176

[33] Cheng D, Liu Y, Zhang Y, et al. Polydopamine-assisted deposition of CuS nanoparticles on cotton fabrics for photocatalytic and photothermal conversion performance. Cellulose, 2020, 27(14): 8443–8455

[34] Ren Y, Yan B, Wang P, et al. Construction of a rapid photothermal antibacterial silk fabric via QCS-guided *in situ* deposition of CuSNPs. ACS Sustainable Chemistry & Engineering, 2022, 10(6): 2192–2203

[35] Kim H J, Choi D I, Lee S, et al. Quick thermal response-transparent-wearable heater based on copper mesh/poly(vinyl alcohol) film. Advanced Engineering Materials, 2021, 23(10): 2100395

[36] Choi J, Byun M, Choi D. Transparent planar layer copper heaters for wearable electronics. Applied Surface Science, 2021, 559: 149895

[37] Kwon M, Kim H, Mohanty A K, et al. Molecular-level contact of graphene/silver nanowires through simultaneous dispersion for a highly stable wearable electrothermal heater. Advanced Materials Technologies, 2021, 6(9): 2100177

[38] Tan C, Dong Z, Li Y, et al. A high performance wearable strain sensor with advanced thermal management for motion monitoring. Nature Communications, 2020, 11(1): 3530

[39] Ma Z, Huang Q, Xu Q, et al. Permeable superelastic liquid-metal fibre mat enables biocompatible and monolithic stretchable electronics. Nature Materials, 2021, 20(6): 859–868

[40] Liu Z, Zheng Y, Jin L, et al. Highly breathable and stretchable strain sensors with insensitive response to pressure and bending. Advanced Functional Materials, 2021, 31(14): 2007622

[41] Gao Q, Kopera B A F, Zhu J, et al. Breathable and flexible polymer membranes with mechanoresponsive electric resistance. Advanced Functional Materials, 2020, 30(26): 1907555

[42] Hong H, Jung Y H, Lee J S, et al. Anisotropic thermal conductive composite by the guided assembly of boron nitride nanosheets for flexible and stretchable electronics. Advanced Functional Materials, 2019, 29(37): 1902575

[43] Cai Q, Scullion D, Gan W, et al. High thermal conductivity of high-quality monolayer boron nitride and its thermal expansion. Science Advances, 2019, 5(6): eaav0129

[44] Guo Y, Qiu H, Ruan K, et al. Hierarchically multifunctional polyimide composite films with strongly enhanced thermal conductivity. Nano-Micro Letters, 2022, 14(1): 26

[45] Chen H, Ginzburg V V, Yang J, et al. Thermal conductivity of

polymer-based composites: fundamentals and applications. Progress in Polymer Science, 2016, 59: 41–85

[46] Burger N, Laachachi A, Ferriol M, et al. Review of thermal conductivity in composites: mechanisms, parameters and theory. Progress in Polymer Science, 2016, 61: 1–28

[47] Wen Z, Wang S, Bao Z, et al. Preparation and oil absorption performance of polyacrylonitrile fiber oil absorption material. Water, Air, and Soil Pollution, 2020, 231(4): 153

[48] Wang Y, Wang W, Liu B, et al. Preparation of durable antibacterial and electrically conductive polyacrylonitrile fibers by copper sulfide coating. Journal of Applied Polymer Science, 2017, 134(44): 45496

[49] Sun Y, Liu Y, Zheng Y, et al. Enhanced energy harvesting ability of ZnO/PAN hybrid piezoelectric nanogenerators. ACS Applied Materials & Interfaces, 2020, 12(49): 54936–54945

[50] Chae H G, Sreekumar T V, Uchida T, et al. A comparison of reinforcement efficiency of various types of carbon nanotubes in polyacrylonitrile fiber. Polymer, 2005, 46(24): 10925–10935

[51] Abdel-Mottaleb M M, Mohamed A, Karim S A, et al. Preparation, characterization, and mechanical properties of polyacrylonitrile (PAN)/graphene oxide (GO) nanofibers. Mechanics of Advanced Materials and Structures, 2020, 27(4): 346–351

[52] Hu S, Zheng Z, Tian Y, et al. Preparation and characterization of electrospun PAN–$CuCl_2$ composite nanofiber membranes with a special net structure for high-performance air filters. Polymers, 2022, 14(20): 4387

[53] Zhang Q, Liu D, Pan W, et al. Flexible stretchable electrothermally/photothermally dual-driven heaters from nano-embedded hierarchical Cu_xS-coated PET fabrics for all-weather wearable thermal management. Journal of Colloid and Interface Science, 2022, 624: 564–578

[54] Dong Y, Xu D, Yu H Y, et al. Highly sensitive, scrub-resistant, robust breathable wearable silk yarn sensors via interfacial multiple covalent reactions for health management. Nano Energy, 2023, 115: 108723

[55] Wang C, Li X, Gao E, et al. Carbonized silk fabric for ultrastretchable, highly sensitive, and wearable strain sensors. Advanced Materials, 2016, 28(31): 6640–6648

[56] He G, Wang L, Bao X, et al. Synergistic flame retardant weft-knitted alginate/viscose fabrics with MXene coating for multifunctional wearable heaters. Composites Part B: Engineering, 2022, 232: 109618

[57] Zhang T, Song B, Li X, et al. Multifunctional hydrophobic MXene-coated cotton fabrics for electro/photothermal conversion, electromagnetic interference shielding, and pressure sensing. ACS Applied Polymer Materials, 2023, 5(8): 6296–6306

[58] Yang Y, Zeng H, Zhou H, et al. Photothermal fabric based on *in situ* growth of CuO@Cu fractal dendrite fiber for personal thermal management. Advanced Engineering Materials, 2023, 25: 2300386

[59] Zhang T, Song B, Li X, et al. *In-situ* twisted spiral fiber with tree-ring like structure for joule heating, photothermal and humidity sensing. Polymer Testing, 2023, 127: 108173

[60] Li H, Wen H, Zhang Z, et al. Reverse thinking of the aggregation-induced emission principle: amplifying molecular motions to boost photothermal efficiency of nanofibers. Angewandte Chemie International Edition, 2020, 59(46): 20371–20375